# Cooperation of Multiple Connected Vehicles at Unsignalized Intersections: Distributed Observation, Optimization, and Control

Yougang Bian, Shengbo Eben Li, *Senior Member, IEEE*, Wei Ren, *Fellow, IEEE*, Jianqiang Wang, Keqiang Li, and Henry X. Liu

***Abstract*—Cooperation of connected vehicles is a promising approach for autonomous intersection control. This article presents a systematic approach to the cooperation of connected vehicles at unsignalized intersections without global coordination. A task-area partition framework is proposed to decompose the mission of cooperative passing into three main tasks, i.e., vehicle state observation, arriving time optimization, and trajectory tracking control. To accomplish these tasks, a distributed observation algorithm is introduced to achieve fixed-time observation of other vehicles' states for passing sequence determination, a distributed optimization algorithm is introduced to schedule conflict-free arriving times for trajectory planning, and a distributed control algorithm is proposed to address parameter mismatches and acceleration saturation for fixed-time trajectory tracking control. Numerical simulations demonstrate that the proposed method can achieve cooperative passing of vehicles without global coordination at the cost of a growth of 8.8–18.1% average travel times in low and medium traffic volumes.**

***Index Terms*—Connected vehicles, cooperation, distributed control, distributed observation, distributed optimization, unsignalized intersection.**

## I. Introduction

RECENT years witness the rise of the connected vehicle technology [1]. With the introduction of vehicle-to-vehicle (V2V) and vehicle-to-infrastructure communication, the behaviors of multiple connected vehicles can be coordinated for global traffic improvement, yielding the so-called cooperative intelligent transportation systems [2].

In the 1-D case, the cooperation of connected vehicles is referred to as platoon control or cooperative adaptive cruise control [3], of which recent typical advances can be found in [4]–[8]. When it comes to urban scenarios, intersections become the main bottlenecks that restrain the application of platoon techniques. In this case, 2-D cooperation becomes necessary, which enables connected vehicles to pass intersections without the coordination of traffic signal lights.

Compared with platoon control that focuses on longitudinal formation, the challenge of 2-D cooperation lies in the strategy design to resolve potential collisions at intersections. To this end, negotiation-based approaches [9], [10] were proposed to resolve collisions by globally reserving spacial and temporal resources for approaching vehicles. Different scheduling mechanisms [11]–[13] were further proposed to improve the "first come, first served" (FCFS) policy [9] commonly used in resource reservation. Moreover, trajectory planning-based methods [14], [15] were also proposed to achieve collision-free passing by eliminating potential trajectory overlaps and cross-collision risks. Note that these methods are based on centralized coordination, which needs global information for decision-making and may bring heavy communication and computation loads. Therefore, decentralized methods were proposed to fill this gap. For example, the virtual platoon method [16] was borrowed in [17] and [18] to transform 2-D vehicle clusters into 1-D virtual platoons for conflict-free passing. Distributed optimal control was studied in [19] to find closed-form solutions in the presence of state and safety constraints, while distributed model predictive control was used in [20] to guarantee provable system-wide safety and liveness. More recent advances in unsignalized intersection control can be found in [21]–[23].

In most of the study on decentralized 2-D cooperation, a global coordinator, which can be either a roadside unit or an approaching vehicle, is still needed for global information sharing or task scheduling. For example, in [19], a roadside coordinator is needed for information sharing; in [17] and [18], a global coordinator is needed for virtual platoon generation. The dependence on global coordination inevitably poses high demands on communication and computation loads and infrastructure

Manuscript received September 28, 2018; revised April 18, 2019 and October 6, 2019; accepted November 12, 2019. Date of publication December 24, 2019; date of current version August 18, 2020. The work of Y. Bian was supported by the China Scholarship Council. This work was supported in part by the National Key R&D Program of China under Grant 2016YFB0100906, in part by the National Science Foundation under Grant ECCS-1920798, and in part by the Open Fund of State Key Laboratory of Automotive Safety and Energy with KF1828. *(Corresponding author: Keqiang Li.)*

Y. Bian, S. E. Li, J. Wang, and K. Li are with the State Key Laboratory of Automotive Safety and Energy, School of Vehicle and Mobility, Tsinghua University, Beijing 100084, China (e-mail: byg10@foxmail.com; lishbo@tsinghua.edu.cn; wjqlws@tsinghua.edu.cn; likq@tsinghua.edu.cn).

W. Ren is with the Department of Electrical and Computer Engineering, University of California at Riverside, Riverside, CA 92521 USA (e-mail: ren@ece.ucr.edu).

H. X. Liu is with the DiDi Chuxing Technology Company Ltd., Beijing 100190, China (e-mail: henryliu@didiglobal.com).

Color versions of one or more of the figures in this article are available online at http://ieeexplore.ieee.org.

Digital Object Identifier 10.1109/TIE.2019.2960757

construction (if roadside units are needed). Some recent studies are dedicated to address this issue. In [24], the conflict resolution is decoupled temporally by iteratively optimizing desired time slots and speed profiles using neighboring vehicles' information. In [25], a consensus-based method is proposed for trajectory optimization through an iterative process. Different from these studies, this article tries to address the abovementioned issue from the multiagent system (MAS) [26], [27] point of view. In an MAS, individual agents interact locally to accomplish global tasks in state estimation [28], optimization [29], [30], and control [31]. By taking connected vehicles as mobile agents with computational and communication capabilities, this study presents a systematic approach to the cooperation of multivehicle systems without global coordination. In detail, we propose a task-area partition framework for task decomposition. Within this framework, distributed observation, optimization, and control algorithms are designed to achieve cooperative passing at an unsignalized intersection without the dependence on global coordination. The contributions of this article include the following.

1) A task-area partition framework is proposed to decompose the mission of cooperative passing at unsignalized intersections into three main tasks, i.e., vehicle state observation, arriving time optimization, and trajectory tracking control.
2) Distributed observation and optimization algorithms are introduced to achieve fixed-time observation of other vehicles' states and to schedule conflict-free arriving times, respectively. These algorithms remove the dependence on global coordination in information sharing and task scheduling.
3) A distributed control algorithm is proposed to guarantee fixed-time tracking of desired trajectories. This control algorithm addresses parameter mismatches and acceleration saturation in longitudinal vehicle dynamics, which are not considered in conjunction in existing works. The fixed-time convergence of tracking errors, which is also not considered in existing studies, improves the trajectory tracking performance to guarantee passing safety at intersections.

The remainder of this article is organized as follows. Section II presents some preliminaries. Section III details the problem statement. Section IV introduces the task-area partition framework and the design of distributed observation, optimization, and control algorithms. Numerical simulations are conducted in Section V. Finally, Section VI concludes this article.

## II. Preliminaries

A directed network is denoted by $\mathcal{G} = (\mathcal{V}, \mathcal{E}, A)$, where $\mathcal{V} = \{V_1, V_2, \dots, V_N\}$ is the set of nodes, $\mathcal{E} \subseteq \mathcal{V} \times \mathcal{V}$ is the set of directed edges, and $A = [a_{ij}] \in \mathbb{R}^{N\times N}$ is the adjacency matrix with $a_{ij}$ being 1, if node $i$ can obtain the information of node $j$, or 0, otherwise. We assume that there is no self-loop in $\mathcal{G}$, i.e., $a_{ii} = 0, \forall i \in \{1, 2, \dots, N\}$, which means node (vehicle) $i$ does not transmit information to itself via communication. The Laplacian matrix associated with $\mathcal{G}$ is denoted by $L = [l_{ij}] \in \mathbb{R}^{N\times N}$, where $l_{ij} = -a_{ij}$ if $i \neq j$, and $l_{ii} = -\sum_{j=1}^{N} a_{ij}$. Graph $\mathcal{G}$ is undirected and connected if $a_{ij} = a_{ji}$ $\forall i, j \in \{1, 2, \dots, N\}$, and there is a path between every pair of nodes.

*Definition 1 (see [32]):* Consider a system

$$\dot{x} = f(x), \quad x(t_0) = x_0 \tag{1}$$

where $x = [x_1, x_2, \dots, x_N]^\top \in \mathbb{R}^N$, $f(x) : \mathbb{R}^N \to \mathbb{R}^N$ is continuous on $\mathbb{R}^N$, and $f(0) = 0$. System (1) is said to achieve *fixed-time stabilization* at the origin if it is asymptotically stable and there exists a settling time $T > t_0$, which is related to $x_0$, and a fixed constant $T_{\max} > T$ such that

$$\begin{cases} \lim_{t\to T^-} x(t) = 0 \\ x(t) = 0 \quad \forall t \geq T \end{cases}.$$

*Lemma 1 (see [32]):* For system (1), suppose that there exists a continuous radially unbounded and positive definite function $V(x) : \mathbb{R}^N \to \mathbb{R}$ and four real numbers $a > 0$, $b > 0$, $0 < p < 1$, and $q > 1$ such that

$$\dot{V}(x) \leq -aV(x)^p - bV(x)^q.$$

Then, system (1) achieves fixed-time stabilization at the origin, and the settling time $T$ satisfies

$$T \leq \frac{1}{a(1-p)} + \frac{1}{b(q-1)}.$$

*Lemma 2 (see [33]):* Let $x_1, x_2, \dots, x_N \geq 0$, $0 < p < 1$, and $q > 1$. Then, it holds that

$$\sum_{i=1}^{N} x_i^p \geq \left(\sum_{i=1}^{N} x_i\right)^p, \quad \sum_{i=1}^{N} x_i^q \geq N^{1-q}\left(\sum_{i=1}^{N} x_i\right)^q.$$

Given a constant $k \geq 0$, for any $x \in \mathbb{R}$, define the function $x^{[k]} = \text{sign}(x)|x|^k$, where $\text{sign}(\cdot)$ is the sign function, i.e., $\text{sign}(x) = 1$, if $x > 0$; $\text{sign}(x) = 0$, if $x = 0$; and $\text{sign}(x) = -1$, if $x < 0$.

*Lemma 3 (see [34]):* Consider an $N$-dimensional $(N \geq 2)$ chain of integrators

$$\begin{aligned} &\dot{x}_1(t) = x_2(t), \quad x_1(t_0) = x_{10} \\ &\dot{x}_2(t) = x_3(t), \quad x_2(t_0) = x_{20} \\ &\dots \\ &\dot{x}_N(t) = u(t), \quad x_N(t_0) = x_{N0} \end{aligned} \tag{2}$$

where $x = [x_1, x_2, \dots, x_N]^\top \in \mathbb{R}^N$ and $u \in \mathbb{R}$. Let the constants $k_{i,j} > 0, i \in \{1, 2, \dots, N\}, j \in \{1, 2\}$, be assigned such that $s^N + k_{N,j}s^{N-1} + \dots + k_{1,j}$ is Hurwitz for any $j \in \{1, 2\}$. In addition, let the constants $\gamma_i$ and $\beta_i$ be selected as follows: $\gamma_i \in (0, 1)$, $i \in \{1, 2, \dots, N\}$, satisfy the recurrent relations $\gamma_{i-1} = \gamma_i\gamma_{i+1}/(2\gamma_{i+1} - \gamma_i)$, $i \in \{2, 3, \dots, N\}$, $\gamma_{N+1} = 1$, and $\gamma_N = \gamma \in (1 - \epsilon_1, 1)$ for a sufficiently small $\epsilon_1 > 0$; $\beta_i > 1$, $i \in \{1, 2, \dots, N\}$, satisfy the recurrent relations $\beta_{i-1} = \beta_i\beta_{i+1}/(2\beta_{i+1} - \beta_i)$, $i \in \{2, 3, \dots, N\}$, $\beta_{N+1} = 1$, and $\beta_N = \beta \in (1, 1 + \epsilon_2)$ for a sufficiently small $\epsilon_2 > 0$. Moreover, let

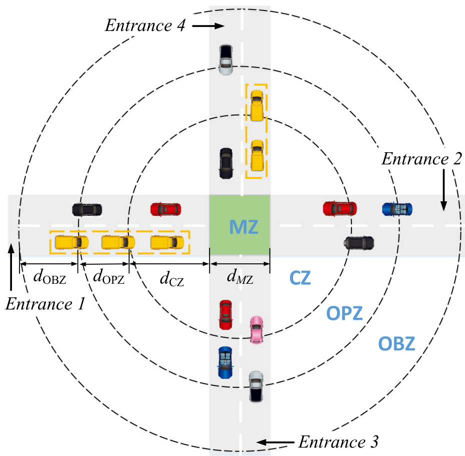


Fig. 1. Partition of the intersection area (OBZ; OPZ; CZ; MZ).

$\varepsilon > 0$ be a constant. Then, system (2) achieves fixed-time stabilization at the origin under the feedback control

$$u = -\varepsilon\left(\sum_{i=1}^{N} k_{i,1} x_i^{[\gamma_i]} + \sum_{i=1}^{N} k_{i,2} x_i^{[\beta_i]}\right)$$

with the settling time upper bounded by

$$T_m(\varepsilon) = \frac{\lambda_{\max}^{\sigma_1}(P_1)}{r_1\sigma_1} + \frac{1}{r_2\sigma_2\Upsilon^{\sigma_2}}$$

where $\sigma_1 = \frac{1-\gamma}{\gamma}$, $\sigma_2 = \frac{\beta-1}{\beta}$, $r_1 = \frac{\lambda_{\min}(Q_1)}{\lambda_{\min}(P_1)}$, $r_2 = \frac{\lambda_{\min}(Q_2)}{\lambda_{\min}(P_2)}$, $\Upsilon \le \lambda_{\min}(P_2)$ is a positive number, and $P_1$, $P_2$, $Q_1$, and $Q_2 \in \mathbb{R}^{N\times N}$ are symmetric positive definite matrices satisfying

$$P_1 A_1 + A_1^T P_1 = -Q_1, \quad P_2 A_2 + A_2^T P_2 = -Q_2$$

with $A_j$, $j \in \{1, 2\}$, being

$$A_j = \begin{pmatrix} 0 & 1 & 0 & \cdots & 0 \\ 0 & 0 & 1 & \cdots & 0 \\ \cdots & & & & \\ 0 & 0 & 0 & \cdots & 1 \\ -\varepsilon k_{1,j} & -\varepsilon k_{2,j} & -\varepsilon k_{3,j} & \cdots & -\varepsilon k_{N,j} \end{pmatrix}.$$

## III. Problem Statement

Consider an unsignalized four-legged intersection shown in Fig. 1. For simplicity, we assume that each intersection leg has only one through lane, so vehicles only go straight without turning movements [19]. The intersection can be simultaneously occupied by more than one vehicle for better travel efficiency, as is considered in [9]. Assume that all vehicles are connected vehicles equipped with navigation and V2V communication devices, so they can measure and share their location and movement information, and their movements are controllable. In addition, we assume no communication time delays or package losses to simplify the problem.

Suppose that all vehicles have satisfactory lane-keeping capability, so we only focus on the longitudinal vehicle control. To balance accuracy and conciseness, we neglect the left–right asymmetry and tire slip and consider the following nonlinear dynamics model, which is similar to the one used in [4] and [5] but has no time lags in the powertrain

$$\dot{p}_i = v_i \tag{3a}$$

$$\dot{v}_i = \frac{\eta_i}{m_i r_i} T_i - \frac{C_{A,i}}{m_i} v_i^2 - (f_i \cos\alpha_{r,i} + \sin\alpha_{r,i}) g \tag{3b}$$

where $p_i$ and $v_i$ are the position and velocity, respectively; $T_i$ and $\eta_i$ are the driving torque (control input) and the mechanical efficiency, respectively, of the driveline; $m_i$ and $r_i$ are the mass and tire radius, respectively; $C_{A,i}$, $f_i$, and $g$ are the coefficients of the aerodynamics drag, rolling resistance, and gravitational acceleration, respectively; $\alpha_{r,i}$ is the slope of the road. Moreover, we make the following assumption.

*Assumption 1:* Vehicles' acceleration $a_i \equiv \dot{v}_i$ is bounded

$$a_m \le a_i \le a_M$$

where $a_m < 0$ and $a_M > 0$ are known constants.

To address the nonlinearity in model (3), we define

$$\theta_{1,i} = \frac{m_i r_i}{\eta_i}, \theta_{2,i} = \frac{C_{A,i}}{m_i}, \theta_{3,i} = f_i \cos\alpha_{r,i} + \sin\alpha_{r,i}$$

and then use the following feedback linearization law:

$$T_i = \hat{\theta}_{1,i}(u_i + \hat{\theta}_{2,i} v_i^2 + \hat{\theta}_{3,i} g) \tag{4}$$

where $\hat{\theta}_{ij}$ is the estimation of $\theta_{i,j}$, $j \in \{1, 2, 3\}$. Under Assumption 1, we substitute (4) into (3) and obtain the following model:

$$\dot{p}_i = v_i \tag{5a}$$

$$\dot{v}_i = \mathrm{sat}_{a_m}^{a_M}\left(\frac{\hat{\theta}_{1,i}}{\theta_{1,i}} u_i + w_i\right) \tag{5b}$$

where $w_i$ is the equivalent disturbance arising from parameter mismatches

$$w_i = \left(\frac{\hat{\theta}_{1,i}}{\theta_{1,i}}\hat{\theta}_{2,i} - \theta_{2,i}\right) v_i^2 + \left(\frac{\hat{\theta}_{1,i}}{\theta_{1,i}}\hat{\theta}_{3,i} - \theta_{3,i}\right) g$$

and $\mathrm{sat}_{a_m}^{a_M}(x) : \mathbb{R} \to \mathbb{R}$ is a saturation function

$$\mathrm{sat}_{a_m}^{a_M}(x) = \begin{cases} a_m & \text{if } x < a_m \\ x & \text{if } a_m \le x \le a_M \\ a_M & \text{if } x > a_M \end{cases}.$$

Model (5) is similar to the one used in [7] but contains parameter mismatches and acceleration saturation.

To sum up, the objective of this article is to design a strategy for the cooperative passing of vehicles with dynamics (5) at the unsignalized intersection shown in Fig. 1. In particular, the task should be fulfilled in a distributed fashion.

## IV. Methodology

This section proposes a task-area partition framework for task decomposition and presents detailed algorithms to accomplish these tasks.

## A. Task-Area Partition Framework

The proposed task-area partition framework decomposes the mission of cooperative passing into three main tasks, i.e., vehicle state observation, arriving time optimization, and trajectory tracking control. In Fig. 1, the intersection area is accordingly partitioned into four zones, i.e., observation zone (OBZ), optimization zone (OPZ), control zone (CZ), and merging zone (MZ), of which the ranges are denoted by $d_{\text{OBZ}}$, $d_{\text{OPZ}}$, $d_{\text{CZ}}$, and $d_{\text{MZ}}$, respectively. In each zone, vehicles are assigned in the following different tasks.

1) First, in the OBZ, approaching vehicles observe all the other approaching vehicles' states, with which the passing sequence is determined.
2) Then, in the OPZ, approaching vehicles optimize their arriving times at the MZ, with which their desired trajectories in the CZ are determined.
3) Next, in the CZ, approaching vehicles track their desired trajectories as well as keeping intervehicle safety gaps so as to arrive at the MZ on time.
4) Finally, in the MZ, approaching vehicles pass the intersection (then they become departing vehicles) and leave the intersection area.

This framework provides a systematic method for the design of multivehicle cooperation systems by assigning sensing, decision, and control tasks to different task areas.

The communication range is denoted by $d_{\text{comm}}$. Two vehicles are called neighbors if the distance between them is less than or equal to $d_{\text{comm}}$. The graph consisting of all the approaching and departing vehicles in the four zones is denoted by $\mathcal{G}$. Then, we make the following assumption.

*Assumption 2:* Graph $\mathcal{G}$ is undirected and connected.

We note that this assumption is realistic when the traffic in the intersection area is not too light so that there are plenty of vehicles in the intersection area to form a connected graph. In fact, this assumption is looser than that of a global coordinator that can communicate with all the approaching vehicles.

## B. Distributed Observation of Vehicle States

Since $d_{\text{comm}}$ is limited, $\mathcal{G}$ may not be a complete graph, i.e., there may exist a pair of vehicles in $\mathcal{G}$ that are not neighbors. Then, in order to determine the passing sequence in a distributed manner, approaching vehicles in the OBZ need to observe each others' states once they enter the OBZ. At the meantime, they are also observed by other vehicles in $\mathcal{G}$.

Assume the number of vehicles in $\mathcal{G}$ is $N+1$. Label with subscript 0 the vehicle to be observed, and $1, 2, \ldots, N$ the other vehicles. Vehicle $i$'s observations of vehicle 0's position and velocity are denoted by $\hat{p}_{0,i}$ and $\hat{v}_{0,i}$, respectively. If vehicle 0 is a neighbor of vehicle $i$, we directly have $\hat{p}_{0,i} = p_0$ and $\hat{v}_{0,i} = v_0$. Otherwise, we call vehicle $i$ a *naive* vehicle. Define $B_{\text{ob}} = \text{diag}\{b_1, b_2, \ldots, b_n\}$, where $n$ is the number of naive vehicles, and $b_i$ equals 1, if vehicle $i$ can acquire information from vehicle 0's neighbors, or 0, otherwise. The subgraph of $\mathcal{G}$ consisting of all the naive vehicles is denoted by $\mathcal{G}_{\text{ob}}$, and the Laplacian matrix of $\mathcal{G}_{\text{ob}}$ is denoted by $L_{\text{ob}}$. Then, we introduce the following distributed observation algorithm [31]:

$$\begin{aligned}
\dot{\hat{p}}_{0,i} &= \hat{v}_{0,i} + \mu_1 \left( \sum_{j=1}^{N} a_{ij}(\hat{p}_{0,j} - \hat{p}_{0,i}) + b_i(p_0 - \hat{p}_{0,i}) \right)^{[q_{\text{ob}}]} \\
&\quad + \nu_1 \text{sign} \left( \sum_{j=1}^{N} a_{ij}(\hat{p}_{0,j} - \hat{p}_{0,i}) + b_i(p_0 - \hat{p}_{0,i}) \right) \\
\dot{\hat{v}}_{0,i} &= \mu_2 \left( \sum_{j=1}^{N} a_{ij}(\hat{v}_{0,j} - \hat{v}_{0,i}) + b_i(v_0 - \hat{v}_{0,i}) \right)^{[q_{\text{ob}}]} \\
&\quad + \nu_2 \text{sign} \left( \sum_{j=1}^{N} a_{ij}(\hat{v}_{0,j} - \hat{v}_{0,i}) + b_i(v_0 - \hat{v}_{0,i}) \right) \quad (6)
\end{aligned}$$

where $\mu_j$ and $\nu_j, j \in \{1, 2\}$ are gains to be designed, and $q_{\text{ob}} > 1$ is an arbitrary constant.

Let the observation errors be $\tilde{p}_{0,i} = \hat{p}_{0,i} - p_0$ and $\tilde{v}_{0,i} = \hat{v}_{0,i} - v_0$, and denote the stacked observation errors by $\tilde{p}_0 = [\tilde{p}_{0,1}, \tilde{p}_{0,2}, \ldots, \tilde{p}_{0,N}]^\top$ and $\tilde{v}_0 = [\tilde{v}_{0,1}, \tilde{v}_{0,2}, \ldots, \tilde{v}_{0,N}]^\top$. Then, the observation error system becomes

$$\begin{aligned}
\dot{\tilde{p}}_0 &= -\mu_1 (L_B \tilde{p}_0)^{[q_{\text{ob}}]} - \nu_1 \text{sign}(L_B \tilde{p}_0) + \tilde{v}_0 \\
\dot{\tilde{v}}_0 &= -\mu_2 (L_B \tilde{v}_0)^{[q_{\text{ob}}]} - \nu_2 \text{sign}(L_B \tilde{v}_0) - \mathbf{1} a_0 \quad (7)
\end{aligned}$$

where $L_B = L_{\text{ob}} + B_{\text{ob}}$, and $\mathbf{1} = [1, 1, \ldots, 1]^\top \in \mathbb{R}^N$. The minimum eigenvalue of $L_B$ is denoted by $\underline{\lambda}_{L_B}$. Then, we make the following assumption and present the first theorem.

*Assumption 3:* In the OBZ, approaching vehicles' velocities are bounded, i.e.,

$$v_m \le v_i \le v_M$$

where $v_m > 0$ and $v_M > 0$ are known constants.

*Theorem 1:* Suppose Assumptions 1–3 hold. For vehicle model (5), if the gains in observer (6) satisfy

$$\begin{aligned}
\mu_j &= \frac{\zeta}{2} \quad \forall j \in \{1, 2\} \\
\nu_1 &= \frac{\zeta}{2} + v_M, \quad \nu_2 = \frac{\zeta}{2} + \max\{|a_m|, a_M\}
\end{aligned}$$

where $\zeta > 0$ is a constant, system (7) achieves fixed-time stabilization at the origin with the settling time upper bounded by

$$T_{\text{ob}} := \frac{1}{\zeta} \left( \frac{N^{\frac{q_{\text{ob}}-1}{2}}}{(q_{\text{ob}} - 1)(2\underline{\lambda}_{L_B})^{\frac{q_{\text{ob}}+1}{2}}} + \frac{1}{(2\underline{\lambda}_{L_B})^{\frac{1}{2}}} \right).$$

*Proof:* Similar to [31]. ■

With the observed vehicle states, the passing sequence $S_p$ can be determined by each approaching vehicle. Note that approaching vehicles that enter the OPZ earlier also appear earlier in $S_p$ and are supposed to enter the MZ earlier.

## C. Distributed Optimization of Arriving Times

When approaching vehicles enter the OPZ, they are going to optimize their arriving times at the MZ according to $S_p$.

Suppose that $S_p = \{1, 2, \ldots, N\}$. The optimization problem for determining the arriving times is formulated as follows.

First, if approaching vehicle $i$ runs with velocity $v_i$ in both the OPZ and CZ until entering the MZ, the arriving time, called the *nominal arriving time*, is

$$t_{\mathrm{MZ}n,i} = t_{\mathrm{OPZ},i} + \frac{d_{\mathrm{OPZ}} + d_{\mathrm{CZ}}}{v_i} \tag{8}$$

where $t_{\mathrm{OPZ},i}$ is the time instant when approaching vehicle $i$ enters the OPZ.

Next, if approaching vehicle $i$ runs with velocity $v_i$ in the OPZ, but accelerates with the maximum acceleration $a_M$ until reaching a given maximum velocity $v_M$ when it enters the CZ, the arriving time, called the *earliest arriving time*, is

$$t_{\mathrm{MZ}e,i} = t_{\mathrm{OPZ},i} + \frac{d_{\mathrm{OPZ}}}{v_i} + \frac{v_M - v_i}{a_M} + \frac{d_{\mathrm{CZ}}}{v_M} - \frac{v_M^2 - v_i^2}{2a_M v_M}. \tag{9}$$

Here, it is assumed that all approaching vehicles can reach velocity $v_M$ before entering the MZ.

Suppose that approaching vehicle $i-k$ $(k > 0)$ is the closest predecessor that has a conflict movement with approaching vehicle $i$, i.e., vehicle $i-k$ may collide with vehicle $i$ in the MZ. The index of vehicle $i-k$ can be determined using the depth-first spanning tree searching algorithm [18]. The *occupancy time* of vehicle $i-k$ is denoted by $t_{\mathrm{MZ}o,i-k}$, i.e., the time duration that the MZ is occupied by vehicle $i-k$. This value can be properly designed to allow more than one vehicle to occupy the intersection simultaneously for better travel efficiency. The arriving times of vehicles $i-k$, $i-1$, and $i$ are denoted by $t_{\mathrm{MZ},i-k}$, $t_{\mathrm{MZ},i-1}$, and $t_{\mathrm{MZ},i}$, respectively, and the aggregated arriving time is denoted by $t_{\mathrm{MZ}} = [t_{\mathrm{MZ},1}, t_{\mathrm{MZ},2}, \ldots, t_{\mathrm{MZ},N}]^\top$. Then, we have the following constraints:

$$g_{1,i}(t_{\mathrm{MZ}}) = t_{\mathrm{MZ},i-k} + t_{\mathrm{MZ}o,i-k} - t_{\mathrm{MZ},i} \le 0 \tag{10a}$$

$$g_{2,i}(t_{\mathrm{MZ}}) = t_{\mathrm{MZ},i-1} - t_{\mathrm{MZ},i} \le 0 \tag{10b}$$

$$h_i(t_{\mathrm{MZ},i}) = t_{\mathrm{MZ}e,i} - t_{\mathrm{MZ},i} \le 0. \tag{10c}$$

Here, constraint (10b) imposes vehicle $i$ to pass the MZ according to the passing sequence. This is consistent with the FCFS policy, which provides a conflict-free passing sequence at a low computation cost. There are also studies on passing sequence optimization, e.g., [11], [12]. However, when the global coordinator is removed, these algorithms need to be implemented on all vehicles to generate a consistent passing sequence in a distributed manner, which will increase the computation load in heavy traffic scenarios. Here, we consider constant occupancy times that are determined based on the intersection layout and traffic flow rate. In practice, these occupancy times can be accurately determined based on vehicles' speed profiles for less conservativeness, which, however, will increase the complexity of the optimization problem.

Then, the cost function in the optimization of arriving times consists of two parts. On the one hand, vehicle $i$ may tend to pass the intersection quickly for better travel efficiency, so the deviation from the earliest arriving time, i.e., $|t_{\mathrm{MZ},i} - t_{\mathrm{MZ}e,i}|$, is minimized. On the other hand, vehicle $i$ may tend to maintain the current velocity for better driving comfort, so the deviation from the nominal arriving time, i.e., $|t_{\mathrm{MZ},i} - t_{\mathrm{MZ}n,i}|$, is minimized. Then, by assigning different weighting coefficients to these two objectives, the cost function becomes

$$f_i(t_{\mathrm{MZ},i}) = \alpha_i (t_{\mathrm{MZ},i} - t_{\mathrm{MZ}e,i})^2 + (1-\alpha_i)(t_{\mathrm{MZ},i} - t_{\mathrm{MZ}n,i})^2 \tag{11}$$

where $\alpha_i \in [0, 1]$ is a coefficient owned by vehicle $i$ to represent its preference between driving comfort (a small $\alpha_i$) and travel efficiency (a big $\alpha_i$). Note that $\alpha_i$ may be nonidentical for different vehicles to represent the diversity.

Finally, the optimization problem of vehicle $i$'s arriving time is formulated as follows.

*Problem 1:*

$$\min_{t_{\mathrm{MZ},i}} \quad f_i(t_{\mathrm{MZ},i}) \tag{12a}$$

$$\text{s.t.}: \quad g_{1,i}(t_{\mathrm{MZ}}) \le 0 \tag{12b}$$

$$g_{2,i}(t_{\mathrm{MZ}}) \le 0 \tag{12c}$$

$$h_i(t_{\mathrm{MZ},i}) \le 0. \tag{12d}$$

For Problem 1, $f_i(t_{\mathrm{MZ},i})$ and $h_i(t_{\mathrm{MZ},i})$ contain only local information, while $g_{1,i}(t_{\mathrm{MZ}})$ and $g_{2,i}(t_{\mathrm{MZ}})$ contain predecessors' information. In detail, $t_{\mathrm{MZ}o,i-k}$ is a static variable, but $t_{\mathrm{MZ},i-k}$ and $t_{\mathrm{MZ},i-1}$ are dynamic variables to be optimized by vehicles $i-k$ and $i-1$, respectively, so they are not available for vehicle $i$ in real time.

To address this issue, we consider the global optimization problem. The subgraph of $\mathcal{G}$ consisting of all approaching vehicles in the OPZ is denoted by $\mathcal{G}_{\mathrm{op}}$, and the Laplacian matrix of $\mathcal{G}_{\mathrm{op}}$ is denoted by $L_{\mathrm{op}}$. Vehicle $i$'s estimation of the optimal solution $t^*_{\mathrm{MZ}}$ to Problem 1 is denoted by $\hat{t}^i_{\mathrm{MZ}} = [\hat{t}^i_{\mathrm{MZ},1}, \hat{t}^i_{\mathrm{MZ},2}, \ldots, \hat{t}^i_{\mathrm{MZ},N}]^\top$. The stacked estimations are denoted by $\hat{t}_{\mathrm{MZ}} = [\hat{t}^{1\top}_{\mathrm{MZ}}, \hat{t}^{2\top}_{\mathrm{MZ}}, \ldots, \hat{t}^{N\top}_{\mathrm{MZ}}]^\top$. A unit vector with the $i$th entry being 1 and the other entries being 0 are denoted by $e_i = [0, 0, \ldots, 1, \ldots, 0]^\top \in \mathbb{R}^N$, and the Kronecker product is denoted by $\otimes$. Then, the global optimization problem is formulated as follows.

*Problem 2:*

$$\min_{\hat{t}_{\mathrm{MZ}}} \quad \sum_{i=1}^{N} f_i(e_i^\top \hat{t}^i_{\mathrm{MZ}}) + \frac{1}{2} \hat{t}^\top_{\mathrm{MZ}} (L_{\mathrm{op}} \otimes I_N) \hat{t}_{\mathrm{MZ}} \tag{13a}$$

$$\text{s.t.}: \quad \hat{t}^i_{\mathrm{MZ}} \in \Omega_i \quad \forall i \in \{1, 2, \ldots, N\} \tag{13b}$$

$$(L_{\mathrm{op}} \otimes I_N) \hat{t}_{\mathrm{MZ}} = 0 \tag{13c}$$

where $\Omega_i$ is the feasible set of $\hat{t}^i_{\mathrm{MZ}}$ defined as

$$\Omega_i = \{t \in \mathbb{R}^N | h_i(e_i^\top t) \le 0, \\ g_{1,k}(t) \le 0, g_{2,k}(t) \le 0 \quad \forall k \in \{1, 2, \ldots, N\}\}.$$

For Problem 2, the first term of cost function (13a) penalizes the sum of vehicles' cost function in Problem 1, while the second term penalizes the disagreement of vehicles' estimations. Moreover, constraint (13c) restricts $\hat{t}_{\mathrm{MZ}}$ to the null space of $L_{\mathrm{op}}$, so that vehicles' estimations achieve consensus, i.e., $\hat{t}^i_{\mathrm{MZ}} = \hat{t}^j_{\mathrm{MZ}}$ $\forall i, j \in \{1, 2, \ldots, N\}$.

For Problem 2, we introduce the following distributed optimization algorithm [29]:

$$\dot{\hat{t}}^i_{\text{MZ}} = P_{\mathcal{T}_{\Omega_i}(\hat{t}^i_{\text{MZ}})}\left(-\alpha_s \sum_{j=1}^N a_{ij}(\hat{t}^i_{\text{MZ}} - \hat{t}^j_{\text{MZ}}) - \alpha_s \sum_{j=1}^N a_{ij}(\mu_i - \mu_j) - e_i \nabla f_i\left(e_i^\top \hat{t}^i_{\text{MZ}}\right)\right) \tag{14a}$$

$$\dot{\mu}_i = \sum_{j=1}^N a_{ij}\left(\hat{t}^i_{\text{MZ}} - \hat{t}^j_{\text{MZ}}\right) \tag{14b}$$

where $\mathcal{T}_{\Omega_i}(\hat{t}^i_{\text{MZ}})$ is the tangent cone of $\Omega_i$ at $\hat{t}^i_{\text{MZ}} \in \Omega_i$, $P_{\mathcal{T}_{\Omega_i}(\hat{t}^i_{\text{MZ}})}(\cdot)$ is the projection operator to $\mathcal{T}_{\Omega_i}(\hat{t}^i_{\text{MZ}})$, and $\alpha_s > 0$ is an arbitrary constant.

In algorithm (14), the set $\Omega_i$ is available for approaching vehicle $i$ since it has accurately observed all the other approaching vehicles' states in the OBZ. Therefore, vehicle $i$ only needs to exchange $\hat{t}^i_{\text{MZ}}$ and $\mu_i$ with its neighbors, which means algorithm (14) can be implemented in a distributed fashion. Then, we present the second theorem.

*Theorem 2:* Suppose that Assumption 2 holds. For Problem 2, algorithm (14) guarantees that the estimated arriving time $\hat{t}^i_{\text{MZ}}$ converges to the optimal one $t^*_{\text{MZ}}$ $\forall i \in \{1, 2, \ldots, N\}$.

*Proof:* See [29]. ■

When approaching vehicles leave the OPZ, the desired arriving times, denoted by $\bar{t}_{\text{MZ},i}$, are obtained and will be used as constraints for vehicle trajectory optimization, which is similar to [35].

## D. Distributed Control of Approaching Vehicles

When approaching vehicles enter the CZ, they are going to adjust their trajectories so as to enter the MZ at $\bar{t}_{\text{MZ},i}$. To this end, each approaching vehicle generates and tracks a desired trajectory $p_{d,i}(t)$, which should avoid trajectory overlaps as well as satisfying the following constraints:

$$\begin{cases} p_{d,i}(t_{\text{CZ},i}) = p_i(t_{\text{CZ},i}) \\ p_{d,i}(\bar{t}_{\text{MZ},i}) = p_i(t_{\text{CZ},i}) + d_{\text{CZ}} \\ v_m \le \dot{p}_{d,i}(t) \le v_M, t \in (t_{\text{CZ},i}, \bar{t}_{\text{MZ},i}) \\ a_{m,0} \le \ddot{p}_{d,i}(t) \le a_{M,0}, t \in (t_{\text{CZ},i}, \bar{t}_{\text{MZ},i}) \end{cases}$$

where $t_{\text{CZ},i}$ is the time instant when approaching vehicle $i$ enters the CZ, and $a_{M,0}$ and $a_{m,0}$ are the upper and lower bounds of desired acceleration, respectively.

In particular, approaching vehicles running in platoons can pass the intersection without being split into single vehicles, as shown in Fig. 1. In this case, only the platoon leader takes part in the optimization and trajectory planning on behalf of all the followers. Index the vehicles in a platoon by $1, 2, \ldots, N$, and define a virtual leader indexed by 0 with trajectory $p_0(t) = p_{d,1}(t) + d_p$, where $d_p > 0$ is the constant desired intervehicle distance. A boolean variable is denoted by $b_i$, which equals 1, if vehicle $i$ can obtain $p_0$, or 0, otherwise. Define neighbor position and velocity errors as

$$e_{i1} = \sum_{j=1}^N a_{ij}(p_i - p_j + (i-j)d_p) + b_i(p_i - p_0 + id_p)$$

$$e_{i2} = \sum_{j=1}^N a_{ij}(v_i - v_j) + b_i(v_i - v_0)$$

then, we have

$$\begin{aligned} \dot{e}_{i1} &= e_{i2} \\ \dot{e}_{i2} &= \sum_{j=1}^N a_{ij}(\dot{v}_i - a_j) + b_i(\dot{v}_i - a_0) \\ &= (d_i + b_i)\dot{v}_i - \left(\sum_{j=1}^N a_{ij}a_j + b_i a_0\right) \\ &= (d_i + b_i)\text{sat}^{a_M}_{a_m}\left(\frac{\hat{\theta}_{1,i}}{\theta_{1,i}}u_i + w_i\right) - \left(\sum_{j=1}^N a_{ij}a_j + b_i a_0\right) \end{aligned} \tag{15}$$

where $d_i = \sum_{j=1}^N a_{ij}$ is the in-degree of vehicle $i$.

Inspired by Lemma 3, we define a sliding mode variable

$$s_i(t) = e_{i2}(t) - \int_{t_{\text{CZ},i}}^t \varepsilon_i u_{ri}(t)\text{d}t \tag{16}$$

where $\varepsilon_i > 0$ is a constant to be designed, and

$$u_{ri} = -\sum_{j=1}^2 k_{j,1} e_{ij}^{[\gamma_j]} - \sum_{j=1}^2 k_{j,2} e_{ij}^{[\beta_j]}$$

where the parameters $k_{j,1}$, $k_{j,2}$, $\gamma_j$, $\kappa_j$, and $\beta_j$, $j \in \{1, 2\}$, are selected as given in Lemma 3. Hence, in order to let $s_i$ converge to 0, the control input is designed as follows:

$$u_i = \frac{1}{d_i + b_i}\left(\sum_{j=1}^N a_{ij}a_j + b_i a_0 + \varepsilon_i u_{ri} - \left(\delta_i(s_i^{[p_c]} + s_i^{[q_c]}) + \rho_i \text{sign}(s_i)\right)\right) \tag{17}$$

where $0 < p_c < 1$ and $q_c > 1$ are arbitrary constants, $\delta_i > 0$ and $\rho_i > 0$ are constants to be designed.

*Assumption 4:* The acceleration of the virtual leading vehicle is bounded, i.e.,

$$a_m < a_{m,0} \le a_0 \le a_{M,0} < a_M$$

where $a_{m,0} < 0$ and $a_{M,0} > 0$ are known constants.

This assumption can be satisfied by properly designing the desired trajectory $p_{d,i}(t)$. Then, we present the third theorem.

*Theorem 3:* Suppose that Assumptions 1, 2, and 4 hold and $b_i = 1, \forall i \in \{1, 2, \ldots, N\}$. For vehicle model (5) and controller

(17), if the following condition holds

$$b_l < \left(\frac{\hat{\theta}_{1,i}}{\theta_{1,i}} - 1\right)\left(\sum_{j=1}^{N} a_{ij}a_i + b_i a_0\right) + (d_i + b_i)w_i < b_u$$
$$\forall i \in \{1, 2, \ldots, N\} \tag{18}$$

where

$$\begin{cases} b_l = a_m - a_{m,0} + \frac{a_M - a_{M,0}}{2}, b_u = \frac{a_M - a_{M,0}}{2} \\ \qquad\qquad \text{if } a_M - a_{M,0} \geq a_{m,0} - a_m \\ b_l = \frac{a_m - a_{m,0}}{2}, b_u = \frac{a_m - a_{m,0}}{2} + a_M - a_{M,0}, \text{otherwise} \end{cases}$$

there exist $\varepsilon_i > 0$, $\delta_i > 0$, and $\rho_i > 0$, such that system (15) achieves fixed-time stabilization at the origin with the settling time upper bounded by

$$T_c := T_s + T_e$$

where

$$T_s := \frac{2}{\min_i\{\delta_i \frac{\hat{\theta}_{1,i}}{\theta_{1,i}}\}}\left(\frac{1}{1-p_c} + \frac{N^{\frac{q_c-1}{2}}}{q_c - 1}\right) \tag{19a}$$

$$T_e := \max_i\{T_m(\varepsilon_i)\} \tag{19b}$$

where $T_m(\varepsilon_i)$ is given in Lemma 3.

*Proof:* We first prove the existence of parameters $\varepsilon_i$, $\delta_i$, and $\rho_i$ when condition (18) holds. By substituting (15) into (16), the time derivative of $s_i$ becomes

$$\begin{aligned} \dot{s}_i &= \dot{e}_{i2} - \varepsilon_i u_{ri} \\ &= (d_i + b_i)\mathrm{sat}_{a_m}^{a_M}\left(\frac{\xi_1 + \xi_2 + \xi_3 + \varepsilon_i u_{ri}}{d_i + b_i}\right) - \xi_1 - \varepsilon_i u_{ri} \\ &= \mathrm{sat}_{(d_i+b_i)a_m}^{(d_i+b_i)a_M}(\xi_1 + \xi_2 + \xi_3 + \varepsilon_i u_{ri}) - \xi_1 - \varepsilon_i u_{ri} \end{aligned} \tag{20}$$

where

$$\xi_1 = \sum_{j=1}^{N} a_{ij}a_j + b_i a_0$$

$$\xi_2 = \left(\frac{\hat{\theta}_{1,i}}{\theta_{1,i}} - 1\right)\left(\sum_{j=1}^{N} a_{ij}a_i + b_i a_0 + \varepsilon_i u_{ri}\right) + (d_i + b_i)w_i$$

$$\xi_3 = -\frac{\hat{\theta}_{1,i}}{\theta_{1,i}}\left(\delta_i(s_i^{[p_c]} + s_i^{[q_c]}) + \rho_i \mathrm{sign}(s_i)\right).$$

Since Assumptions 1 and 4 hold, we have

$$d_i a_m + b_i a_{m,0} \leq \xi_1 \leq d_i a_M + b_i a_{M,0}. \tag{21}$$

In addition, since condition (18) holds, there exists a sufficiently small constant $\varepsilon_{i1} > 0$ such that $\forall \varepsilon_i \in (0, \varepsilon_{i1}]$, it holds that

$$b_l < \xi_2 < b_u. \tag{22}$$

Moreover, by choosing a proper $\rho_i$ such that

$$\frac{\hat{\theta}_{1,i}}{\theta_{1,i}}\rho_i = \sup\|\xi_2\| + \Delta_i \tag{23}$$

where $\Delta_i > 0$ is a constant, we have

$$\xi_3 = -\mathrm{sign}(s_i)(\sup|\xi_2| + \Delta_i) - \delta_i\frac{\hat{\theta}_{1,i}}{\theta_{1,i}}\left(s_i^{[p_c]} + s_i^{[q_c]}\right).$$

When $\Delta_i$ is sufficiently small, there exists a sufficiently small constant $\delta_i > 0$ such that

$$-\max\{|b_l|, b_u\} \leq \xi_3 \leq \max\{|b_l|, b_u\}. \tag{24}$$

Then, by combining (21), (22), and (24), we have

$$(d_i + b_i)a_m < \xi_1 + \xi_2 + \xi_3 < (d_i + b_i)a_M. \tag{25}$$

Then, there exists a sufficiently small constant $\varepsilon_{i2} > 0$ such that $\forall \varepsilon_i \in (0, \min\{\varepsilon_{i1}, \varepsilon_{i2}\}]$, it holds that

$$(d_i + b_i)a_m < \xi_1 + \xi_2 + \xi_3 + \varepsilon_i u_{ri} < (d_i + b_i)a_M. \tag{26}$$

This means that the $\mathrm{sat}_{(d_i+b_i)a_m}^{(d_i+b_i)a_M}(\cdot)$ function in (20) is never saturated. Therefore, (20) becomes

$$\dot{s}_i = (\xi_1 + \xi_2 + \xi_3 + \varepsilon_i u_{ri}) - \xi_1 - \varepsilon_i u_{ri} = \xi_2 + \xi_3.$$

Next, we prove the fixed-time stabilization at the origin. Consider the following Lyapunov function candidate:

$$V_s = \frac{1}{2}\sum_{i=1}^{N} s_i^2.$$

The time derivative of $V_s$ is

$$\begin{aligned} \dot{V}_s &= \sum_{i=1}^{N} s_i \dot{s}_i \\ &\leq -\sum_{i=1}^{N} s_i\left(\delta_i\frac{\hat{\theta}_{1,i}}{\theta_{1,i}}\left(s_i^{[p_c]} + s_i^{[q_c]}\right)\right) \\ &= -\sum_{i=1}^{N} \delta_i\frac{\hat{\theta}_{1,i}}{\theta_{1,i}}\left((s_i^2)^{\frac{p_c+1}{2}} + (s_i^2)^{\frac{q_c+1}{2}}\right) \\ &\leq -\min_i\left\{\delta_i\frac{\hat{\theta}_{1,i}}{\theta_{1,i}}\right\}\left(V_s^{\frac{p_c+1}{2}} + N^{\frac{1-q_c}{2}}V_s^{\frac{q_c+1}{2}}\right). \end{aligned}$$

Here, condition (23) and Lemma 2 are used to derive the first and second inequalities, respectively. Then, according to Lemma 1, $\forall i \in \{1, 2, \ldots, N\}$, $s_i$ converges to 0 in $T_s$ given in (19a). Once $s_i$ converges to 0, we have

$$\dot{e}_{i2}(t) = \varepsilon_i u_{ri}(t).$$

Then, according to Lemma 3, $e_{i1}$ and $e_{i2}$ converge to 0 with the settling time upper bounded by $T_e$ given in (19b).

Therefore, the total settling time is upper bounded by $T_c$ given in (19). ■

In controller (17), $\delta_i$ and $\varepsilon_i$ should be sufficiently small to avoid acceleration saturation. This facilitates the stability analysis, however, brings conservativeness to the convergence rate. In practice, these parameters should be selected properly to improve the convergence rate.

*Remark 1:* The upper bounds of settling times $T_{\mathrm{ob}}$ and $T_c$ are related to the communication topologies, which make them difficult to accurately calculate ahead of time. However, they

TABLE I
SIMULATION PARAMETERS

| Geometry parameters [m] | | | | | | |
|---|---|---|---|---|---|---|
| $d_{\text{OBZ}}$ | $d_{\text{OPZ}}$ | $d_{\text{CZ}}$ | $d_{\text{MZ}}$ | $d_{\text{veh}}$ | $d_p$ | $d_{\text{comm}}$ |
| 50 | 50 | 150 | 8 | 4 | 10 | 300 |

| Vehicle dynamics parameters | | | |
|---|---|---|---|
| Parameter | Unit | True value | Estimated value |
| $m_i$ | kg | 1800 $\sim$ 2200 | 2000 |
| $\eta_i$ | - | 0.82 $\sim$ 0.88 | 0.85 |
| $r_i$ | m | 0.23 $\sim$ 0.27 | 0.25 |
| $C_{\text{A},i}$ | N·s$^2$/m$^2$ | 0.32 $\sim$ 0.38 | 0.35 |
| $f_i$ | - | 0.012 $\sim$ 0.018 | 0.015 |
| $\alpha_{r,i}$ | rad | -0.03 $\sim$ 0.03 | 0 |
| $[a_m, a_M]$ | m/s$^2$ | [-3, 3] | - |

| Observation and optimization parameters | | | | | | |
|---|---|---|---|---|---|---|
| $\mu_1, \mu_2$ | $\nu_1$ | $\nu_2$ | $q_{\text{ob}}$ | $\alpha_i$ | $\alpha_s$ | $[v_m, v_M]$ |
| 0.25 | 5.0 | 1.5 | 1.5 | 0 $\sim$ 1 | 1 | [0,13] m/s |

| Control parameters | | | | | | | | | | | | |
|---|---|---|---|---|---|---|---|---|---|---|---|---|
| $\varepsilon_i$ | $k_{1,1}$ | $k_{2,1}$ | $k_{1,2}$ | $k_{2,2}$ | $\gamma_1$ | $\gamma_2$ | $\beta_1$ | $\beta_2$ | $\delta_i$ | $\rho_i$ | $p_c$ | $q_c$ |
| 0.4 | 0.5 | 1 | 0.5 | 1 | 0.90 | 0.95 | 1.11 | 1.05 | 2 | 1 | 0.8 | 1.2 |

can still give some insights to determine the ranges of the OBZ and CZ. For example, we can set $d_{\text{OBZ}} = v_M \cdot \max\{T_{\text{ob}}\}$ and $d_{\text{CZ}} = v_M \cdot \max\{T_c\}$, where $\max\{T_{\text{ob}}\}$ and $\max\{T_c\}$ can be determined by using historical data of communication topologies. In practice, $d_{\text{OBZ}}$ and $d_{\text{CZ}}$, as well as $d_{\text{OPZ}}$, need to be fine-tuned to guarantee the convergence of algorithms.

## V. Numerical Simulation

In the simulation, we set $t_{\text{MZ}o,i-k} = \frac{d_{\text{MZ}}+d_{\text{veh}}}{v_n} + \frac{d_p}{v_n} N_{f,i-k}$, where $d_{\text{veh}}$ is the vehicle length, $v_n$ is a nominal vehicle speed, and $N_{f,i-k}$ is the number of vehicles that follow vehicle $i-k$ as a platoon. Here, we set $v_n = 8$ m/s since the minimum vehicle speed in the MZ in the simulation turn out to be greater than 9 m/s. The desired trajectory is selected as $p_{d,i}(t) = p_i(t_{\text{CZ},i}) + \frac{t - t_{\text{CZ},i}}{t_{\text{MZ},i} - t_{\text{CZ},i}} d_{\text{CZ}}$ so as to satisfy Assumption 4 as well as to avoid trajectory overlaps. $\text{sign}(\cdot)$ in algorithms (6) and (17) are replaced with $\text{sat}^1_{-1}(\cdot)$ to mitigate chattering effects. $\alpha_i$ is randomly initialized following a uniform distribution between 0 and 1. $q_{\text{ob}}$, $p_c$, and $q_c$ are fine-tuned to balance the convergence performance and chattering effects. Other simulation parameters, as listed in Table I, are selected through trial-and-error to achieve the satisfactory performance. Communication time delays and package losses are neglected here for theoretical validation.

First, the effectiveness of the proposed method is validated in a medium total traffic volume of 2400 veh/h without vehicle platoons. Simulation results are shown in Figs. 2–4. In Fig. 2, the observations tracked the true states well in the OBZ, which guarantee the consistency of $S_p$. The chattering effect arises from the $\text{sat}(\cdot)$ function in discrete-time simulation, and can

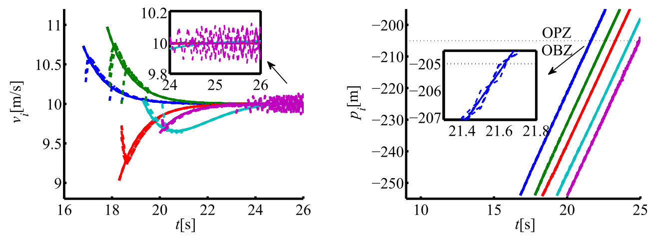

(a) (b)

Fig. 2. State observation profiles in the OBZ (solid lines: true values; dashed lines: observations; different colors: different vehicles). (a) Velocity observations. (b) Position observations.

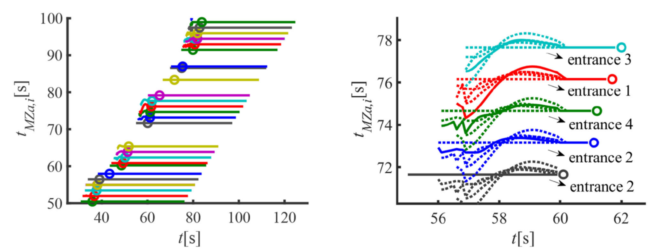

(a) (b)

Fig. 3. Arriving time profiles in the OPZ (solid lines: private values; dashed lines: neighbors' estimations; marker "o": $t_{\text{CZ},i}$; different colors: different vehicles). (a) Evolution trajectories. (b) Consensus process.

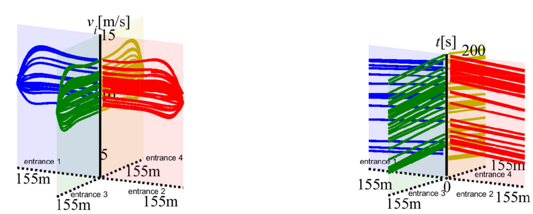

(a) (b)

Fig. 4. Vehicle state profiles in the CZ (different colors: vehicles from different entrances). (a) Velocity profiles. (b) Position profiles.

be mitigated via further parameter fine-tuning. From Fig. 3(a), it is observed that conflict-free arriving times were obtained before approaching vehicles entered the CZ at $t_{\text{CZ},i}$. The consensus process of estimated optimal arriving times shown in Fig. 3(b) further demonstrates the satisfying convergence rate of the distributed optimization algorithm. Fig. 4 illustrates the velocity and position profiles of approaching vehicles from four entrances of the intersection. It is observed that approaching vehicles reached steady velocities in the CZ and entered the MZ orderly. Moreover, the average time cost for one iteration of the optimization algorithm is less than 10 ms, and the average iteration number is less than 50. This demonstrates the real-time performance of the proposed optimization algorithm.

Next, the control performance of the proposed fixed-time platoon controller is compared with the linear platoon controller used in a recent related work [18], which also addresses decentralized cooperation at unsignalized intersections but needs

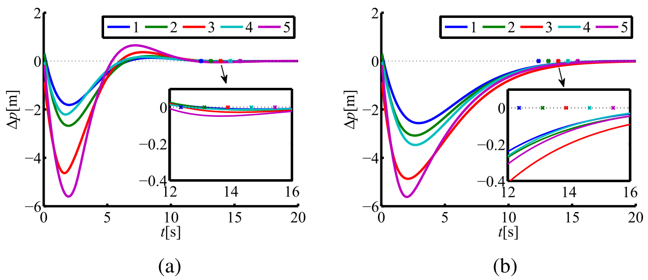

Fig. 5. Comparison of the control performance (marker "x": $\bar{t}_{\mathrm{MZ},i}$). (a) Fixed-time controller. (b) Linear controller [18].

TABLE II
COMPARISON OF AVERAGE TRAVEL TIMES

| Total traffic volume [veh/h] | | 1200 | 2400 | 3600 |
|---|---|---|---|---|
| Travel time [s] | reservation | 20.4 | 21.4 | 23.6 |
| | virtual platoon | 19.6 | 20.5 | 28.3 |
| | proposed | 22.2 | 24.2 | 31.4 |
| Growth rate | reservation | 8.8% | 13.1% | 33.1% |
| | virtual platoon | 13.3% | 18.1% | 15.9% |

global coordination. In the comparison, a platoon of five vehicles were considered to track their desired trajectories in the CZ. As shown in Fig. 5, the fixed-time controller has higher convergence rate than the linear one, which guarantees lower position errors at the desired arriving time $\bar{t}_{\mathrm{MZ},i}$.

Finally, the proposed method is compared with two benchmarks, i.e., the reservation-based method [9] and virtual platoon-based method [18]. In this case, we set $\alpha_i = 1$ to achieve the best travel efficiency. The average travel times of 100 vehicles in 3 different traffic volumes are shown in Table II. It is observed that the proposed method increases the average travel times by 8.8–18.1% in low and medium traffic volumes. This is acceptable considering the cost reduction from removing global coordination. When it comes to a high traffic volume, the average travel times is increased by up to 33.1%, which demonstrates the weakness of the proposed method in high traffic volumes.

## VI. CONCLUSION

This article studied the cooperation of multiple connected vehicles at unsignalized intersections with focus on removing the dependance on global coordination. To this end, a task-area partition framework was proposed for task decomposition, and distributed observation, optimization, and control algorithms were designed for the vehicle state observation, arriving time optimization, and trajectory tracking control tasks, respectively. The observation and optimization algorithms remove the dependence on global coordination in information sharing and task scheduling, while the control algorithm addressed parameter mismatches and acceleration saturation in longitudinal vehicle dynamics and guarantees fixed-time convergence. Simulation results demonstrated that the proposed method can achieve cooperative passing of vehicles without global coordination. A growth of about 8.8–18.1% average travel times in low and medium traffic volumes was also observed in the performance comparison, which is acceptable considering the cost reduction from removing global coordination.

This article only considered vehicles' through movements. In the case of turning movements, vehicles' turning intentions need to be transmitted with V2V communication in the observation stage, then the conflict relationship tree [18] can be used to determine the closest conflicting predecessors for arriving time optimization. In the future work, we are going to study the traffic-demand-adaptive cooperation method for dynamic adjustment of zone ranges to remove the assumption of a connected graph. It is also an interesting topic to extend this method to the case of multiple adjacent unsginalized intersections (e.g., [36] and [37]) and mixed traffic flow environments where human-driven vehicles and autonomous vehicles coexist. Moreover, the FCFS policy needs to be improved to address asymmetric traffic demands [38], and the selection of the occupancy time also deserves further study to balance efficiency and safety.

## REFERENCES


[1] D. Dorrell, A. Vinel, and D. Cao, "Connected vehicles—Advancements in vehicular technologies and informatics," *IEEE Trans. Ind. Electron.*, vol. 62, no. 12, pp. 7824–7826, Dec. 2015.

[2] K. Sjoberg, P. Andres, T. Buburuzan, and A. Brakemeier, "Cooperative intelligent transport systems in Europe: Current deployment status and outlook," *IEEE Veh. Technol. Mag.*, vol. 12, no. 2, pp. 89–97, Jun. 2017.

[3] S. E. Li *et al.*, "Dynamical modeling and distributed control of connected and automated vehicles: Challenges and opportunities," *IEEE Intell. Transp. Syst. Mag.*, vol. 9, no. 3, pp. 46–58, Fall 2017.

[4] J. W. Kwon and D. Chwa, "Adaptive bidirectional platoon control using a coupled sliding mode control method," *IEEE Trans. Intell. Transp. Syst.*, vol. 15, no. 5, pp. 2040–2048, Oct. 2014.

[5] F. Gao, X. Hu, S. E. Li, K. Li, and Q. Sun, "Distributed adaptive sliding mode control of vehicular platoon with uncertain interaction topology," *IEEE Trans. Ind. Electron.*, vol. 65, no. 8, pp. 6352–6361, Aug. 2018.

[6] S. E. Li, F. Gao, K. Li, L.-Y. Wang, K. You, and D. Cao, "Robust longitudinal control of multi-vehicle systems—A distributed H-infinity method," *IEEE Trans. Intell. Transp. Syst.*, vol. 19, no. 9, pp. 2779–2788, Sep. 2018.

[7] Y. Li, C. Tang, S. Peeta, and Y. Wang, "Integral-sliding-mode braking control for connected vehicle platoon: Theory and application," *IEEE Trans. Ind. Electron.*, vol. 66, no. 6, pp. 4618–4628, Jun. 2019.

[8] Y. Bian, Y. Zheng, W. Ren, S. E. Li, J. Wang, and K. Li, "Reducing time headway for platooning of connected vehicles via V2V communication," *Transp. Res. Pt. C-Emerg. Technol.*, vol. 102, pp. 87–105, 2019.

[9] K. Dresner and P. Stone, "A multiagent approach to autonomous intersection management," *J. Artif. Intell. Res.*, vol. 31, pp. 591–656, 2008.

[10] S. Huang, A. W. Sadek, and Y. Zhao, "Assessing the mobility and environmental benefits of reservation-based intelligent intersections using an integrated simulator," *IEEE Trans. Intell. Transp. Syst.*, vol. 13, no. 3, pp. 1201–1214, Sep. 2012.

[11] L. Li and F. Y. Wang, "Cooperative driving at blind crossings using intervehicle communication," *IEEE Trans. Veh. Technol.*, vol. 55, no. 6, pp. 1712–1724, Nov. 2006.

[12] K. Zhang, D. Zhang, A. de La Fortelle, X. Wu, and J. Grégoire, "State-driven priority scheduling mechanisms for driverless vehicles approaching intersections," *IEEE Trans. Intell. Transp. Syst.*, vol. 16, no. 5, pp. 2487–2500, Oct. 2015.

[13] W. Wu, J. Zhang, A. Luo, and J. Cao, "Distributed mutual exclusion algorithms for intersection traffic control," *IEEE Trans. Parallel Distrib. Syst.*, vol. 26, no. 1, pp. 65–74, Jan. 2015.

[14] J. Lee and B. Park, "Development and evaluation of a cooperative vehicle intersection control algorithm under the connected vehicles environment," *IEEE Trans. Intell. Transp. Syst.*, vol. 13, no. 1, pp. 81–90, Mar. 2012.

[15] M. A. S. Kamal, J. Imura, T. Hayakawa, A. Ohata, and K. Aihara, "A vehicle-intersection coordination scheme for smooth flows of traffic without using traffic lights," *IEEE Trans. Intell. Transp. Syst.*, vol. 16, no. 3, pp. 1136–1147, Jun. 2015.

[16] A. Uno, T. Sakaguchi, and S. Tsugawa, "A merging control algorithm based on inter-vehicle communication," in *Proc. IEEE/IEEJ/JSAI Int. Conf. Intell. Transp. Syst.*, 1999, pp. 783–787.

[17] A. I. M. Medina, N. van de Wouw, and H. Nijmeijer, "Cooperative intersection control based on virtual platooning," *IEEE Trans. Intell. Transp. Syst.*, vol. 19, no. 6, pp. 1727–1740, Jun. 2018.

[18] B. Xu *et al.*, "Distributed conflict-free cooperation for multiple connected vehicles at unsignalized intersections," *Transp. Res. Pt. C-Emerg. Technol.*, vol. 93, pp. 322–334, 2018.

[19] A. A. Malikopoulos, C. G. Cassandras, and Y. J. Zhang, "A decentralized energy-optimal control framework for connected automated vehicles at signal-free intersections," *Automatica*, vol. 93, pp. 244–256, 2018.

[20] K. Kim and P. R. Kumar, "An MPC-based approach to provable system-wide safety and liveness of autonomous ground traffic," *IEEE Trans. Autom. Control*, vol. 59, no. 12, pp. 3341–3356, Dec. 2014.

[21] L. Chen and C. Englund, "Cooperative intersection management: A survey," *IEEE Trans. Intell. Transp. Syst.*, vol. 17, no. 2, pp. 570–586, Feb. 2016.

[22] J. Rios-Torres and A. A. Malikopoulos, "A survey on the coordination of connected and automated vehicles at intersections and merging at highway on-ramps," *IEEE Trans. Intell. Transp. Syst.*, vol. 18, no. 5, pp. 1066–1077, May 2017.

[23] Y. Meng, L. Li, F.-Y. Wang, K. Li, and Z. Li, "Analysis of cooperative driving strategies for nonsignalized intersections," *IEEE Trans. Veh. Technol.*, vol. 67, no. 4, pp. 2900–2911, Apr. 2018.

[24] C. Liu, C.-W. Lin, S. Shiraishi, and M. Tomizuka, "Distributed conflict resolution for connected autonomous vehicles," *IEEE Trans. Intell. Veh.*, vol. 3, no. 1, pp. 18–29, Mar. 2018.

[25] A. Mirheli, M. Tajalli, L. Hajibabai, and A. Hajbabaie, "A consensus-based distributed trajectory control in a signal-free intersection," *Transp. Res. Pt. C-Emerg. Technol.*, vol. 100, pp. 161–176, 2019.

[26] R. Olfati-Saber, J. A. Fax, and R. M. Murray, "Consensus and cooperation in networked multi-agent systems," *Proc. IEEE*, vol. 95, no. 1, pp. 215–233, Jan. 2007.

[27] W. Ren and Y. Cao, *Distributed Coordination of Multi-Agent Networks: Emergent Problems, Models, and Issues*. Berlin, Germany: Springer, 2010.

[28] S. Wang and W. Ren, "On the convergence conditions of distributed dynamic state estimation using sensor networks: A unified framework," *IEEE Trans. Control Syst. Technol.*, vol. 26, no. 4, pp. 1300–1316, Jul. 2018.

[29] X. Zeng, P. Yi, and Y. Hong, "Distributed continuous-time algorithm for constrained convex optimizations via nonsmooth analysis approach," *IEEE Trans. Autom. Control*, vol. 62, no. 10, pp. 5227–5233, Oct. 2017.

[30] Y. Zhu, W. Yu, G. Wen, G. Chen, and W. Ren, "Continuous-time distributed subgradient algorithm for convex optimization with general constraints," *IEEE Trans. Autom. Control*, vol. 64, no. 4, pp. 1694–1701, Apr. 2019.

[31] Z. Zuo, B. Tian, M. Defoort, and Z. Ding, "Fixed-time consensus tracking for multiagent systems with high-order integrator dynamics," *IEEE Trans. Autom. Control*, vol. 63, no. 2, pp. 563–570, Feb. 2018.

[32] A. Polyakov, "Nonlinear feedback design for fixed-time stabilization of linear control systems," *IEEE Trans. Autom. Control*, vol. 57, no. 8, pp. 2106–2110, Aug. 2012.

[33] Z. Zuo and L. Tie, "A new class of finite-time nonlinear consensus protocols for multi-agent systems," *Int. J. Control*, vol. 87, no. 2, pp. 363–370, 2014.

[34] M. Basin, Y. Shtessel, and F. Aldukali, "Continuous finite- and fixed-time high-order regulators," *J. Franklin Inst.*, vol. 353, no. 18, pp. 5001–5012, 2016.

[35] B. Xu *et al.*, "Cooperative method of traffic signal optimization and speed control of connected vehicles at isolated intersections," *IEEE Trans. Intell. Transp. Syst.*, vol. 20, no. 4, pp. 1390–1403, Apr. 2019.

[36] M. Tajalli and A. Hajbabaie, "Distributed optimization and coordination algorithms for dynamic speed optimization of connected and autonomous vehicles in urban street networks," *Transp. Res. Pt. C-Emerg. Technol.*, vol. 95, pp. 497–515, 2018.

[37] Y. J. Zhang, A. A. Malikopoulos, and C. G. Cassandras, "Optimal control and coordination of connected and automated vehicles at urban traffic intersections," in *Proc. Amer. Control Conf.*, 2016, pp. 6227–6232.

[38] M. W. Levin, S. D. Boyles, and R. Patel, "Paradoxes of reservation-based intersection controls in traffic networks," *Transp. Res. Pt. A-Policy Pract.*, vol. 90, pp. 14–25, 2016.


**Yougang Bian** received the the B.E. degree in automotive engineering and the Ph.D. degree in mechanical engineering from Tsinghua University, Beijing, China, in 2014 and 2019, respectively.

From 2017 to 2018, he was a Visiting Student with the Department of Electrical and Computer Engineering, University of California at Riverside, Riverside, CA, USA. His research focuses on cooperative control and distributed control with their applications to connected and automated vehicles.

Dr. Bian was the recipient of the Best Paper Award in the IEEE Intelligent Vehicles Symposium 2017.

**Shengbo Eben Li** (M'11–SM'17) received the M.S. and Ph.D. degrees in mechanical engineering from Tsinghua University, Beijing, China, in 2006 and 2009, respectively.

He was with the Stanford University, Stanford, CA, USA, University of Michigan, Ann Arbor, MI, USA, and University of California, Berkeley, Berkeley, CA, USA. He is currently Tenured Associate Professor with the School of Vehicle and Mobility, Tsinghua University. He is the author of more than 100 peer-reviewed journal/conference papers, and the coinventor of more than 20 Chinese patents. His research focuses on intelligent vehicles and driver assistance, driver behavior data mining, distributed learning and control, optimal control and estimation, etc.

He was the recipient of Best Paper Awards in the IEEE Conference on Intelligent Transportation Systems 2014 and 14th ITS Asia-Pacific Forum, National Award for Technological Invention in China (2013), Excellent Young Scholar of National Natural Science Foundation of China (2016), and Young Professorship of Changjiang Scholar Program (2016).

Dr. Li is currently the Technical Programme Committee Member of the IEEE Intelligent Vehicles Symposium, ISC Member of FAST-zero 2017 in Japan, Associated Editor for the IEEE INTELLIGENT TRANSPORTATION SYSTEMS MAGAZINE and IEEE TRANSACTIONS ON INTELLIGENT TRANSPORTATION SYSTEM, etc.

**Wei Ren** (F'16) received the Ph.D. degree in electrical engineering from Brigham Young University, Provo, UT, USA, in 2004.

He is currently a Professor with the Department of Electrical and Computer Engineering, University of California, Riverside (UC Riverside), Riverside, CA, USA. Prior to joining UC Riverside, he was a Faculty Member with the Utah State University, Logan, UT, USA, and a Postdoctoral Research Associate with the University of Maryland, College Park, College Park, MD, USA. His research focuses on distributed control of multiagent systems and autonomous control of unmanned vehicles.

Dr. Ren was a recipient of the IEEE Control Systems Society Antonio Ruberti Young Researcher Prize (2017) and the National Science Foundation CAREER Award (2008). He is currently an Associate Editor for the *Automatica* and IEEE TRANSACTIONS ON AUTOMATIC CONTROL.

**Jianqiang Wang** received the B.Tech. and M.S. degrees in automotive application engineering from the Jilin University of Technology, Changchun, China, in 1994 and 1997, respectively, and the Ph.D. degree in vehicle operation engineering from Jilin University, Changchun, in 2002.

He is currently a Professor with the School of Vehicle and Mobility, Tsinghua University, Beijing, China. He has authored more than 40 journal papers and is currently a coholder of 30 patent applications. His research focuses on intelligent vehicles, driving assistance systems, and driver behavior.

Dr. Wang was a recipient of the Best Paper Awards in IEEE Intelligent Vehicles (IV) Symposium, 2014, IEEE IV 2017, 14th ITS Asia-Pacific Forum, the Distinguished Young Scientists of National Science Foundation China, in 2016, and the New Century Excellent Talents, in 2008.

**Keqiang Li** received the B.S. degree in automotive engineering from Tsinghua University, Beijing, China, in 1985, the M.S. and Ph.D. degrees in mechanical engineering from Chongqing University, Chongqing, China, in 1988 and 1995, respectively.

He was with the Japanese and Germany Automotive Companies and Academic Institutions for many years including Tokyo University of Agriculture and Technology, Fuchu, Japan, and the University of Tokyo, Tokyo, Japan, Aachen University of Technology, Aachen, Germany, and Isuzu Automobile Corp., Tokyo. He is currently a Professor with the School of Vhicle and Mobility, Tsinghua University, Beijing, China, and also the Director of State Key Laboratory of Automotive Safety and Energy. He has authored about 200 journal/conference papers and is a coinventor of more than 80 patents in China and Japan. He is leading the National Key Project on ICVs (Intelligent and Connected Vehicles) in China. His research focuses on automotive control systems, driver assistance systems, and networked dynamics and control.

Dr. Li was a recipient of Changjiang Scholar Program Professor, National Award for Technological Invention in China, etc.

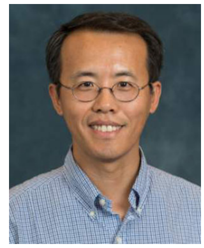

**Henry X. Liu** received the bachelor's degree in automotive engineering from Tsinghua University, Beijing, China, in 1993 and the Ph.D. degree in civil and environmental engineering from the University of Wisconsin-Madison, Madison, WI, USA, in 2000.

He was an Associate Professor of Civil Engineering at the University of Minnesota, Twin Cities, Minneapolis, MN, USA. He is currently a Professor in Civil and Environmental Engineering with the University of Michigan, Ann Arbor, MI, USA, and a Research Professor with the University of Michigan Transportation Research Institute, Ann Arbor. He is also with DiDi Chuxing Technology Company Ltd., Beijing, China. His research focuses on traffic network monitoring, modeling, and control.

Dr. Liu is a Managing Editor of *Journal of Intelligent Transportation Systems* and an Associate Editor of *Transportation Research Part C: Emerging Technologies*. He is also on the Editorial Board of *Transportation Research Part B: Methodological*, *Networks and Spatial Economics*, *Transportmetrica B: Transport Dynamics*, and *IET Intelligent Transport Systems*.